Original Article

Assessing right ventricular peak strain in myocardial infarction patients with mitral regurgitation by cardiac magnetic resonance feature tracking

Xiaoling Wen[1,2#], Yue Gao[1#], Yingkun Guo[3], Yi Zhang[4], Yan Zhang[2], Ke Shi[1], Yuan Li[1], Zhigang Yang[1]

[1]Department of Radiology, West China Hospital, Sichuan University, Chengdu, China; [2]Department of Radiology, West China School of Public Health and West China Fourth Hospital, Sichuan University, Chengdu, China; [3]Department of Radiology, West China Second University Hospital, Sichuan University, Chengdu, China; [4]Department of Radiology, Sichuan Cancer Hospital and Institute, Sichuan Cancer Center, School of Medicine, University of Electronic Science and Technology of China, Chengdu, China

Contributions: (I) Conception and design: Z Yang; (II) Administrative support: Y Li, Y Guo; (III) Provision of study materials or patients: Y Zhang, K Shi; (IV) Collection and assembly of data: X Wen; (V) Data analysis and interpretation: X Wen, Y Gao; (VI) Manuscript writing: All authors; (VII) Final approval of manuscript: All authors.

[#]These authors contributed equally to this work.

Correspondence to: Zhigang Yang, PhD. Department of Radiology, West China Hospital, Sichuan University, 37# Guoxue Xiang, Chengdu 610041, China. Email: yangzg666@163.com.

Background: Although it is known that mitral regurgitation (MR) in patients with myocardial infarction (MI) may increase the right ventricular (RV) afterload, leading to RV dysfunction, the exact detrimental effects on RV function and myocardial peak strain remain unresolved. In this study, we assessed the impact of MR on the impairment of RV myocardial deformation in patients with MI and explored the independent influential factors of RV peak strain.

Methods: A total of 199 MI participants without or with MR were retrospectively assessed in this study. The cardiovascular magnetic resonance examination protocol included a late gadolinium-enhanced (LGE) imaging technique and a cine-balanced steady-state free precession sequence. Statistical tests, including two independent sample *t*-test or Mann-Whitney U-test, analysis of variance, Kruskal-Wallis test, and multiple linear regression analysis models were performed.

Results: The MI (MR+) group exhibited significantly lower RV strain parameters in the radial, circumferential and longitudinal directions when compared to the control and the MI (MR–) groups (both $P<0.05$). The RV global longitudinal peak strain (GLPS) in the MI group significantly decreased when compared with that in the control group ($P<0.05$). As moderate-severe MR worsened in patients with MI, RV myocardial global peak strain and the peak systolic strain rate (PSSR) gradually decreased. Multiple linear regression analysis revealed that left ventricular (LV) GLPS, triglycerides, and age were independently correlated with RV GLPS (all $P<0.05$). RV end-systolic volume (RVESV) acted as an independent association factor for RV global peak strain.

Conclusions: MR may exacerbate the impairment of RV peak strain and functions in patients with MI. LV GLPS was positively correlated with RV GLPS. However, RVESV, triglycerides, and age acted as independent risk factors associated with worsening RV GLPS.

Keywords: Myocardial infarction (MI); mitral regurgitation (MR); right ventricular strain (RV strain); cardiac magnetic resonance feature tracking (CMR-FT); biventricular interaction

Submitted Sep 23, 2023. Accepted for publication Feb 22, 2024. Published online Mar 28, 2024.
doi: 10.21037/qims-23-1360
View this article at: https://dx.doi.org/10.21037/qims-23-1360

Introduction

Over the past few decades, the prognosis and prompt clinical treatment of myocardial infarction (MI) have rapidly improved. However, the development of mitral regurgitation (MR) in patients with MI poses an increased risk of adverse cardiovascular events, including congestive heart failure (HF) and long-term mortality (1). Initially, the right ventricular (RV) function remains intact in patients with MI and MR. However, with the failure of left ventricular (LV) functions, the likelihood of pulmonary hypertension increases, resulting in an elevated RV afterload, which ultimately leads to RV remodeling and dysfunction. The RV function has been identified as a significant predictor of HF development and mortality in patients with MI following LV insufficiency (2). RV systolic dysfunction is associated with serious complications in the short-term period aftermath of MI (3). Furthermore, RV dysfunction plays a crucial role in the development of multi-system organ failure and mortality associated with HF (4). Currently, the RV strain parameters, as assessed using cardiac magnetic resonance feature tracking (CMR-FT) technology are widely utilized for evaluating various cardiac diseases, such as pulmonary hypertension, different cardiomyopathies, and connective tissue diseases (5,6). However, there is a scarcity of studies investigating RV strain in patients with MI by using CMR-FT (7). Magnetic resonance imaging provides a more precise evaluation of MR severity than echocardiography (8). Therefore, we aimed to evaluate global RV deformation and function in patients with MI and MR by using CMR-FT. In addition, we explored the significant risk factors contributing to RV global strain and biventricular interaction effect in patients with MI and MR. We present this article in accordance with the STROBE reporting checklist (available at https://qims.amegroups.com/article/view/10.21037/qims-23-1360/rc).

Methods

Study population

The study was conducted in accordance with the Declaration of Helsinki (as revised in 2013). Ethical approval for this clinical study was obtained from the Biomedical Research Ethics Committee of the West China Hospital of Sichuan University (No. 2019-756). The requirement for informed consent from patients was waived due to the retrospective nature of this study. A total of 623 continuous adult participants diagnosed with MI from January 2010 to September 2022 were retrospectively recruited. The inclusion criteria were the universal definition diagnostic criteria for MI (9-11). The exclusion criteria included the presence of other valvular heart diseases and cardiomyopathy of other causes, arrhythmia, renal function insufficiency (glomerular filtration rate <30 mL/min/1.73 m^2), contraindications for cardiac magnetic resonance (CMR), poor image quality for analysis, a history of lung disease, and presence of RV MI. We employed CMR to diagnose regurgitation of each valve in patients with MI. In our study, MI was more often noted in patients with multiple valve regurgitation, such as MR, tricuspid regurgitation, and aortic regurgitation. Ultimately, only 85 patients with MI and MR were included in the study. A total of 199 age- and sex-matched patients with MI [MI with MR (MR+) *vs.* MI without MR (MR–): 85 (71 males) *vs.* 114 (91 males)] were found to be eligible for this study. Another 89 normal participants (64 males and 25 females) without a history of cardiovascular and other diseases, abnormal results on electrocardiography, and individuals who had undergone CMR imaging were selected for the control group by using the picture archiving and communication system (PACS). The baseline clinical characteristics of all participants were collected. The laboratory data of patients were acquired at nearly the CMR scanning time, which was approximately 1–2 weeks. Diabetes mellitus was defined as the fasting plasma glucose level of ≥7.0 mmol/L with at least an 8-h fasting or post-load glucose level of ≥11.1 mmol/L. Hypertension was defined as diastolic blood pressure (DBP) ≥90 mmHg and/or systolic blood pressure (SBP) ≥140 mmHg for ≥3 times, not on the same day or including patients with antihypertensive medications. Patients with a drinking history were defined as those who consumed alcohol.

CMR-scanning protocols

All patients underwent CMR scanning using a 3.0 T

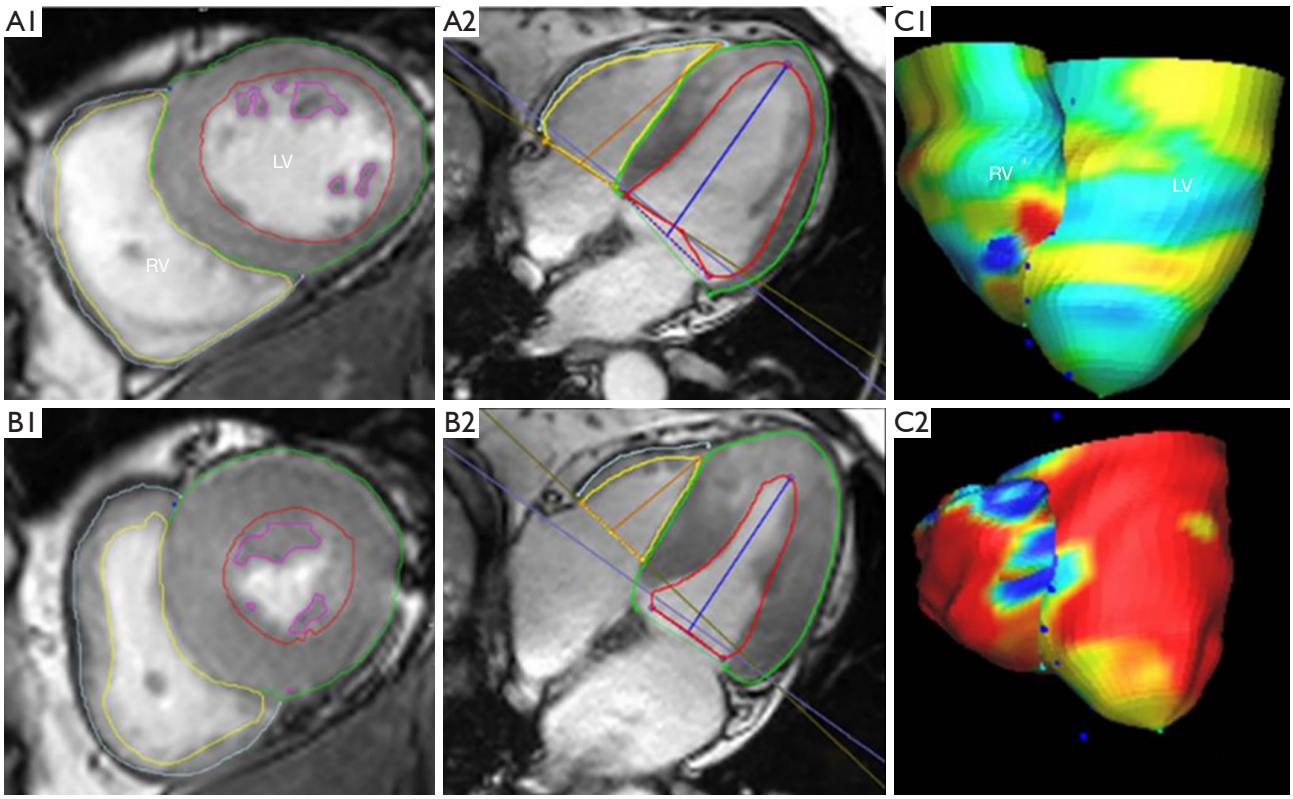

Figure 1 Schematic representation of the cardiac volume and function analyses of LV and RV. (A1,A2) The end-diastolic cine images; (B1,B2) the end-systolic cine images. The red line outlines the endocardium of LV. The green line outlines the epicardium of LV. The purple lines outlines papillary muscles. The yellow line outlines the endocardium of RV. The blue line outlines the epicardium of RV. (C1,C2) Shows the left and right ventricular three-dimensional volume model (C1, end-diastole; C2, end-systole). LV, left ventricle; RV, right ventricle.

whole-body scanner in the supine position (Trio Tim, Siemens Medical Solutions, Erlangen, Germany; Skyra, Siemens Medical Solutions) with a 32-channel phased-array body coil. Cine images were acquired under end-expiratory breath-holding using the steady-state free precession sequence technique, including 2-, 3-, and 4-chamber long-axis cine series of the LV, 2-chamber short-axis cine series of the LV, as well as 4-chamber long-axis cine series, and a 2-chamber short-axis cine series of the RV. Imaging parameters included a viewing area of 240×300 mm^2/288×360 mm^2, matrix size of 192×162/208×139, repetition time/echo time of 2.6–2.8 msec/1.22–1.23 msec, and flip angle of 42°/50°.

Late gadolinium-enhanced (LGE) images were obtained using the phase-sensitive inversion recovery (PSIR) sequence technique (field of view 240×300 mm^2/288 × 360 mm^2; repetition time/echo time of 750 msec/1.18 msec; 512 msec/1.24 msec; flip angle 20°/40°) after an intravenous administration at 2.5–3.0 mL/s, with a dose of 0.2 mL/kg gadolinium-based contrast agent.

Image and data analysis

All CMR images were analyzed using the semi-automated CVI-42 version software (Circle Cardiovascular Imaging, Inc., Calgary, Canada) by two experienced radiologists. The software was employed to manually delineate the endocardial and epicardial traces of RV and LV at end-diastole and end-systole phases in all LV short-axis 2-chamber cine images and 4-chamber long-axis cine images (*Figure 1*). Automated calculations were then performed to acquire the LV and RV global peak strains (GPS), peak diastolic strain rate (PDSR), and peak systolic strain rate (PSSR) in radial, circumferential, and longitudinal directions. GPS includes global radial peak strain (GRPS), global circumferential peak strain (GCPS),

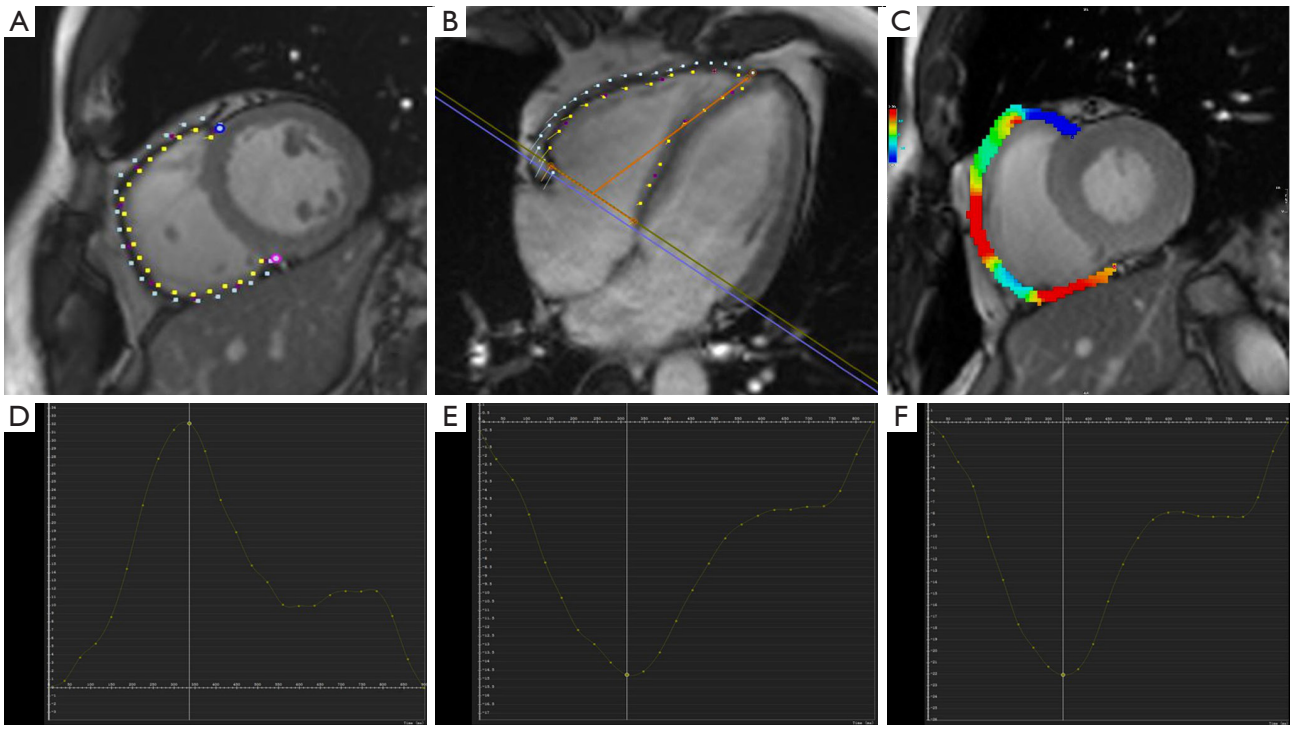

Figure 2 CMR-FT measured the global peak strain of RV in a normal subject. (A,B) Show the trace of the right ventricular endo-and epicardium. The yellow line outlines the endocardium of RV. The blue line outlines the epicardium of RV. (C) Shows the pseudocolor image of the right ventricular radial myocardial strain. (D) Shows the GPS of a normal subject: GRPS =32.1%; (E) GCPS =–14.8%; (F) GLPS =–22.0%. CMR-FT, cardiac magnetic resonance feature tracking; RV, right ventricle; GPS, global peak strain; GRPS, global radial peak strain; GCPS, global circumferential peak strain; GLPS, global longitudinal peak strain.

and global longitudinal peak strain (GLPS). The RV strains were delineated on the 2-chamber short-axis and 4-chamber long-axis cine images (*Figure 2*).

The LV strains were delineated on the 2-chamber short axis and 2- and 4-chamber long-axis cine images. Various cardiac function parameters were obtained, including the stroke volume of the RV (RVSV) and LV (LVSV), mass of the LV (LV mass) and RV (RV mass), ejection fraction of the LV (LVEF) and RV (RVEF), end-diastolic volume of the LV (LVEDV) and RV (RVEDV), and end-systolic volume of the LV (LVESV) and RV (RVESV). The RV cine sequence comprised 8–12 adjacent short-axis images parallel to the plane of the atrioventricular valve. The entire length of the RV was covered in these images, with the contour of the pulmonary valve visible, but not extending beyond the level from the tricuspid annulus to the right apex tracking point. We then carefully excluded the RV papillary muscles and accommodative tracts, and RV trabeculae were ignored.

Diagnosis of MR was facilitated by observing black retrograde blood flow from the LV to left atrium (LA) during the LV systole phase on cine images (2-chamber, 4-chamber long-axis, and short-axis views) (12). Without any other valvular regurgitation or shunt, the MR fraction (MRF) was calculated using the formula: MRF = (LVSV – RVSV)/LVSV × 100%. Based on the MRF results, we defined a mild group (28 cases, MRF <30%), a moderate group (37 cases, 30%≤ MRF <50%), and a severe group (20 cases, MRF ≥50%) (13,14).

To analyze the MI size of LV, the MI regions were categorized into anterior, inferior, and lateral walls based on the bull's eye plot of short-axis images (15). MI diagnosis was confirmed according to the presence of signal intensity exceeding five standard deviations (SD) above the normal myocardium on a short-axis image acquired by using the LGE sequence (16).

Statistical analyses

Statistical analyses for this study were conducted using SPSS software version 26.0 (IBM Corporation, Armonk,

NY, USA), and the graphs were generated by using the GraphPad Prism version 9 for Windows (GraphPad Software Inc., San Diego, CA, USA).

Categorical data were presented as numbers and percentages, with comparisons made using Pearson's Chi-squared test. Normally distributed data were expressed as mean ± SD, and comparisons were conducted using either two independent sample *t*-test or Bonferroni's post-hoc test after analysis of variance.

For data with skewed distributions, the Mann-Whitney nonparametric or Kruskal-Wallis tests were employed, and expressed as median (25–75% interquartile range). Pearson's or Spearman's correlation analysis was utilized to investigate factors associated with RV myocardial strain. Multiple linear regression analyses were employed to identify independent factors associated with RV strain in the MI (MR+) group and assess the biventricular interaction.

Results

Baseline characteristics of participants

In patients with MI, body mass index (BMI) was significantly higher than in controls (P<0.05). Significant differences in SBP (126.88±18.38 mmHg) and resting heart rate [78.50 (67.00, 92.00) bpm] were observed in patients with MI (MR–) relative to those with the controls. No statistically significant differences were noted between the MI group and controls for sex and age (P>0.05). The implementation of primary percutaneous coronary intervention (PCI) in the MI (MR–) group exhibited a significantly higher level than the MI (MR+) group (P<0.05). Laboratory tests revealed that troponin in patients with MI (MR+) was significantly lower than in patients with MI (MR–) (P<0.05). Patients with MI and MR exhibited a significantly higher incidence of diabetes mellitus [30 cases (35.3%) *vs.* 17 cases (14.9%)] than patients with MI without MR (P<0.05) (*Table 1*).

Analyses of RV and LV function parameters

Patients with MI (MR+) exhibited significantly higher RVESV [54.58 (38.09, 64.48) Ml] and RV mass [24.46 (19.47, 28.45) g] than normal participants and patients with MI (MR–), whereas RVEDV was similar to that of controls. RVEF [48.60 (40.53, 56.28)%] and RVSV (51.65± 18.19 mL) in patients with MI (MR+) were significantly reduced compared to that in patients with MI (MR–) and in controls (all P<0.05). Patients with MI (MR+) showed significantly higher LVEDV [212.89 (165.62, 264.17) mL], LVESV [129.50 (86.51, 188.67) mL], LV mass [114.71 (95.76, 133.07) g], and lower LVEF (38.46%±13.57%) than patients with MI (MR–) and controls (*Table 2*). The lateral region and the infarct size of MI in patients with MR were higher than that in patients without regurgitation (all P<0.05, *Table 2*).

RV and LV peak strain differences between the groups

In patients with MI (MR+), RV GPS (radial, 16.25%±7.74%; circumferential, −9.69%±4.33% longitudinal, −14.57%±5.16%), PSSR [radial, 0.93±0.43 s^{-1}; circumferential, −0.59±0.33 s^{-1}; longitudinal, −1.02 (−1.42, −0.81) s^{-1}], and PDSR [radial, −0.78 (−1.07, −0.52) s^{-1}; longitudinal, 0.98 (0.72, 1.43) s^{-1}] were significantly reduced when compared with that in the MI (MR–) group (all P<0.05). RV GPS (radial, 19.64%±8.85%; longitudinal, −16.59%±5.58%) of the MI (MR–) group significantly decreased when compared with that in the normal group (all P<0.05). In the MI (MR–) group, RV PSSR [−1.30 (−1.62, −0.99) s^{-1}] and PDSR [1.17 (0.88, 1.53)] s^{-1} increased compensatory in the longitudinal direction when compared to the controls (all P<0.05). LV GPS in three directions (i.e., radial, circumferential, and longitudinal) of the MI (MR+) group were all significantly lower than those in the control and MI (MR–) groups (all P<0.05, *Table 3*). *Figure 3* indicates the measurement of RV GPS and the peak strain rate parameters in patients with MI with or without MR.

RV strain changes in patients with MI with different degrees of MR

Among patients with MI and MR, 33.0% exhibited mild MR (28 cases), 43.5% exhibited moderate MR (37 cases), and 23.5% exhibited severe MR (20 cases). The global PSSR (radial: 0.94±0.42 s^{-1}; circumferential: −0.59±0.35 s^{-1}) and PDSR [longitudinal: 0.88 (0.73, 1.48) s^{-1}] of patients with MI and moderate MR was significantly reduced when compared with those in patients with MI without MR. The GPS (radial: 12.36%±7.71%; longitudinal: −11.65%±3.50%) and PSSR [radial: 0.66 (0.31, 0.88) s^{-1} and circumferential: −0.47±0.28 s^{-1}] of the MI (MR+, severe) group were significantly reduced when compared with those in the MI (MR+, mild) and MI (MR–) groups (*Table 4*).

Table 1 Clinical baseline characteristics of the normal control group and MI patients with/without MR groups

Characteristics	Normal control subjects (n=89)	MI	
		MR– (n=114)	MR+ (n=85)
BMI, kg/m^2	22.29 (20.35, 24.65)	24.83±3.43*	25.26 (22.49, 26.06)*
SBP, mmHg	119.96±9.47	126.88±18.38*	117.26±19.89$^{\Delta}$
Male	64 (71.9)	91 (79.8)	71 (83.5)
Age, years	53.68±10.57	55.79±13.17	54.75±13.12
Rest heart rate, bpm	72.54±11.08	78.50 (67.00, 92.00)*	76.00 (67.00, 87.00)
Time from infarct to CMR, days	–	6.66 (3.25, 34.50)	12.41 (3.45, 54.41)
Infarct size, LV hyperenhancement %	–	24.63 (14.27, 35.04)	35.70 (23.24, 48.45)*
Pain to balloon time, hours	–	8.0 (5.0, 72.0)	18.0 (5.0, 108.0)
Primary PCI		93 (81.6)	59 (69.4)$^{\Delta}$
Fasting plasma glucose, mmol/L	–	6.02 (5.23, 7.14)	6.20 (5.46, 8.68)
Total cholesterol, mmol/L	–	4.20±1.01	3.80 (3.14, 4.58)
Triglycerides, mmol/L	–	1.53 (1.07, 2.26)	1.41 (0.99, 2.17)
Troponin, ng/L	–	930.00 (54.75, 2,876.00)	85.90 (18.05, 1,832.00)$^{\Delta}$
Risk factors			
Diabetes mellitus	–	17 (14.9)	30 (35.3)$^{\Delta}$
Smoking	–	72 (63.2)	61 (71.8)
Hypertension	–	58 (50.9)	40 (47.1)
Drinking	–	46 (40.4)	25 (29.4)
Medications drugs			
Aspirin/clopidogrel	–	103 (90.4)	76 (89.4)
Statins	–	101 (88.6)	73 (85.9)
Beta-blocker	–	78 (68.4)	54 (63.5)
ACEI/ARB	–	53 (46.5)	47 (55.3)
Biguanides	–	9 (7.9)	15 (17.6)$^{\Delta}$

Data are presented as mean ± standard deviation, or the median (25th, 75th percentile), or number (percentage). *, MI patients *vs.* controls (P<0.05); $^{\Delta}$, MI (MR+) group *vs.* MI (MR–) group (P<0.05). MI, myocardial infarction; MR, mitral regurgitation; MR–, without mitral regurgitation; MR+, with mitral regurgitation; BMI, body mass index; SBP, systolic blood pressure; CMR, cardiac magnetic resonance; LV, left ventricle; PCI, percutaneous coronary intervention; ACEI/ARB, angiotensin-converting enzyme inhibitor/angiotensin II receptor blocker.

Factors influencing RV GPS in patients with MI and MR

Negative correlations were observed among the MRF and RV GRPS (r=–0.334, P=0.002), GCPS (r=–0.281, P=0.010), and GLPS (r=–0.283, P=0.009) in patients with MI and MR. In addition, in patients with MI and MR, negative correlations were observed between the MI size and RV GPS (GRPS: r=–0.291, P=0.007; GCPS: r=–0.257, P=0.018), but there was no significant correlation with GLPS (r=–0.072, P=0.515). Moreover, in patients with MI and MR, LV GPS (i.e., radial, circumferential, and longitudinal) and LVEF were negatively correlated with RV GPS (i.e., radial, circumferential, and longitudinal) (*Table 5*).

Multivariate linear regression analyses, adjusted for sex, resting heart rate, BMI, age, SBP, and included clinical baseline data between different MI groups (all P<0.1), as

Table 2 Comparison of the function parameters of the left and right ventricle and infarct distribution regions of LV between myocardial infarction patients with/without mitral regurgitation and the control groups

Parameters	Normal controls (n=89)	MI	
		MR– (n=114)	MR+ (n=85)
RV function			
RVEDV, mL	119.21±32.89	107.56±29.23	112.36±31.57
RVESV, mL	52.23±18.76	48.72±17.94	54.58 (38.09, 64.48)*$^{\Delta}$
RVSV, mL	66.98±17.01	58.84±19.35*	51.65±18.19*$^{\Delta}$
RVEF (%)	56.68±5.63	54.75±10.81	48.60 (40.53, 56.28)*$^{\Delta}$
RV mass, g	20.28 (16.51, 24.33)	20.16 (16.46, 24.58)	24.46 (19.47, 28.45)*$^{\Delta}$
LV function			
LVEDV, mL	123.03±25.91	162.92±41.30*	212.89 (165.62, 264.17)*$^{\Delta}$
LVESV, mL	42.70 (36.17, 52.68)	86.67±36.15*	129.50 (86.51, 188.67)*$^{\Delta}$
LVSV, mL	77.78±17.37	76.24±19.74	78.97±18.92
LVEF, %	63.00±6.26	50.44 (40.37, 55.50)*	38.46±13.57*$^{\Delta}$
LV mass, g	74.93±18.89	105.89±26.12*	114.71 (95.76, 133.07)*$^{\Delta}$
Infarct distribution regions of LV			
Anterior region	–	75 (65.8)	53 (62.4)
Lateral region	–	32 (28.1)	49 (57.6)*
Inferior region	–	52 (45.6)	42 (49.4)
Infarct size, LV hyperenhancement %	–	24.63 (14.27, 35.04)	35.70 (23.24, 48.45)*

Data are presented as mean ± standard deviation, or the median (25th, 75th percentile), or number (percentage). A patient has a single, two or three-walled myocardial infarction. *, P<0.05, the MI group was compared with the normal control group; $^{\Delta}$, P<0.05, MI (MR+) patients were compared with MI (MR–) patients. LV, left ventricle; MI, myocardial infarction; MR–, without mitral regurgitation; MR+, with mitral regurgitation; RV, right ventricle; EDV/ESV, end-diastolic/end-systolic volume; SV/EF, stroke volume/ejection fraction.

well as time from infarct to CMR, MI location, coronary artery stent, and risk factors of patients with MI, indicating that LV GLPS was an independent indicator of RV GLPS (β=0.224, P=0.029) in patients with MI and MR. RVESV was an independent indicator of RV GPS (radial, circumferential, and longitudinal, all P<0.05) (*Table 6*). Age and triglycerides acted as independent indicators of RV GLPS (all P<0.05). *Figure 4* displays a scatter plot demonstrating the relationship between LV GPS and RV GPS.

Discussion

In this study, we scrutinized the effects of MR on cardiac structure, function, and RV strain in patients with MI. Our key findings were as follows: (I) the MI (MR–) group exhibited diminished RV stroke volume, radial, and longitudinal peak strain before circumferential peak strain changes. Longitudinal PSSR and PDSR indicated compensatory increases. (II) In patients with MI (MR+), RV myocardial strain parameters, including radial and circumferential and longitudinal GPS, PDSR (except for circumferential PDSR), and PSSR were further compromised, accompanied by a significant decrease in RVEF. (III) Relative to patients with MI (MR–), RV PSSR was significantly impaired in patients with MI (MR+, moderate). RV GPS and PSSR in patients with MI (MR+, severe) were further reduced when compared to MI (MR–) and MI (MR+, mild) groups, exacerbating systolic function damage. (IV) LV GLPS was independently correlated with RV GLPS in patients with MI and MR. RVESV was an independent factor associated with RV GPS. Age and triglycerides were independent indicators of RV GLPS.

Table 3 Comparison of the strain parameters of LV and RV between MI patients with/without MR and control groups

Parameters	Normal controls (n=89)	MI	
		MR– (n=114)	MR+ (n=85)
RV PS, %			
Radial	24.92±9.59	19.64±8.85*	16.25±7.74*$^{\Delta}$
Circumferential	–12.23±3.59	–11.41±4.27	–9.69±4.33*$^{\Delta}$
Longitudinal	–19.24±5.27	–16.59±5.58*	–14.57±5.16*$^{\Delta}$
RV PSSR, s^{-1}			
Radial	1.25 (0.93, 1.70)	1.10 (0.87, 1.55)	0.93±0.43*$^{\Delta}$
Circumferential	–0.69 (–0.95, –0.53)	–0.76 (–0.95, –0.62)	–0.59±0.33*$^{\Delta}$
Longitudinal	–1.00 (–1.25, –0.77)	–1.30 (–1.62, –0.99)*	–1.02 (–1.42, –0.81)$^{\Delta}$
RV PDSR, s^{-1}			
Radial	–1.27 (–1.63, –1.03)	–0.87 (–1.21, –0.65)*	–0.78 (–1.07, –0.52)*$^{\Delta}$
Circumferential	0.69 (0.57, 0.82)	0.59 (0.44, 0.69)*	0.54±0.31*
Longitudinal	1.02 (0.86, 1.27)	1.17 (0.88, 1.53)*	0.98 (0.72, 1.43)$^{\Delta}$
LV PS, %			
Radial	37.23±8.56	21.68±8.61*	16.75±7.94*$^{\Delta}$
Circumferential	–20.33±2.74	–13.96±5.00*	–11.39±4.65*$^{\Delta}$
Longitudinal	–14.56±2.89	–9.13±4.39*	–7.56±3.42*$^{\Delta}$

Data are presented as mean ± standard deviation, or the median (25th, 75th percentile). *, P<0.05, the MI group was compared with the normal control group; $^{\Delta}$, P<0.05, the MI (MR+) group compared with the MI (MR–) group. LV, left ventricle; RV, right ventricle; MI, myocardial infarction; MR, mitral regurgitation; MR–, without mitral regurgitation; MR+, with mitral regurgitation; PS, peak strain; PSSR, peak systolic strain rate; PDSR, peak diastolic strain rate.

Research status of RV myocardial strain

The intricate anatomy and asymmetric morphology of the RV make evaluating RV function and biomechanical changes challenging. MR feature tracking enables reproducible assessment of myocardial strain of RV cardiomyopathy (17). RV GLPS is a robust predictor of RV dysfunction with good reproducibility (18). RV longitudinal strain holds significant clinical value across various diseases, including cardiomyopathies, congenital heart diseases, coronary artery disease, and connective tissue diseases (6). As HF progresses, both longitudinal and circumferential myocardial global strain decline (19). A cutoff value of –20% for RV GLPS demonstrates 70% sensitivity and 79% specificity in identifying RV dysfunction (18). CMR imaging is the reference standard for non-invasive assessment of RV functions (20). Myocardial deformation analysis offers biomechanical insights into myocardial scarring, with CMR imaging increasingly serving as a tool to assess the RV structure and function.

Characteristics of RV myocardial strain in patients with MI

RV cell apoptosis markedly increased despite that the RV wall was not ischemic in patients with cardiac remodeling after acute MI (21). In MI with anterior ST-segment elevation, RV dysfunction serves as an independent predictor of recurrent MI, cardiogenic shock, long-term hospitalization, and mortality (22).

Antoni *et al.* reported that RV myocardial strain reduction is a robust independent predictor of clinical adverse events in patients with MI (23). Our study on the risk factors revealed a higher incidence of diabetes mellitus in patients with MI (MR+), suggesting potential exacerbation of the condition in patients with MI. In addition, our study found that the RV stroke volume in patients with MI (MR–) was

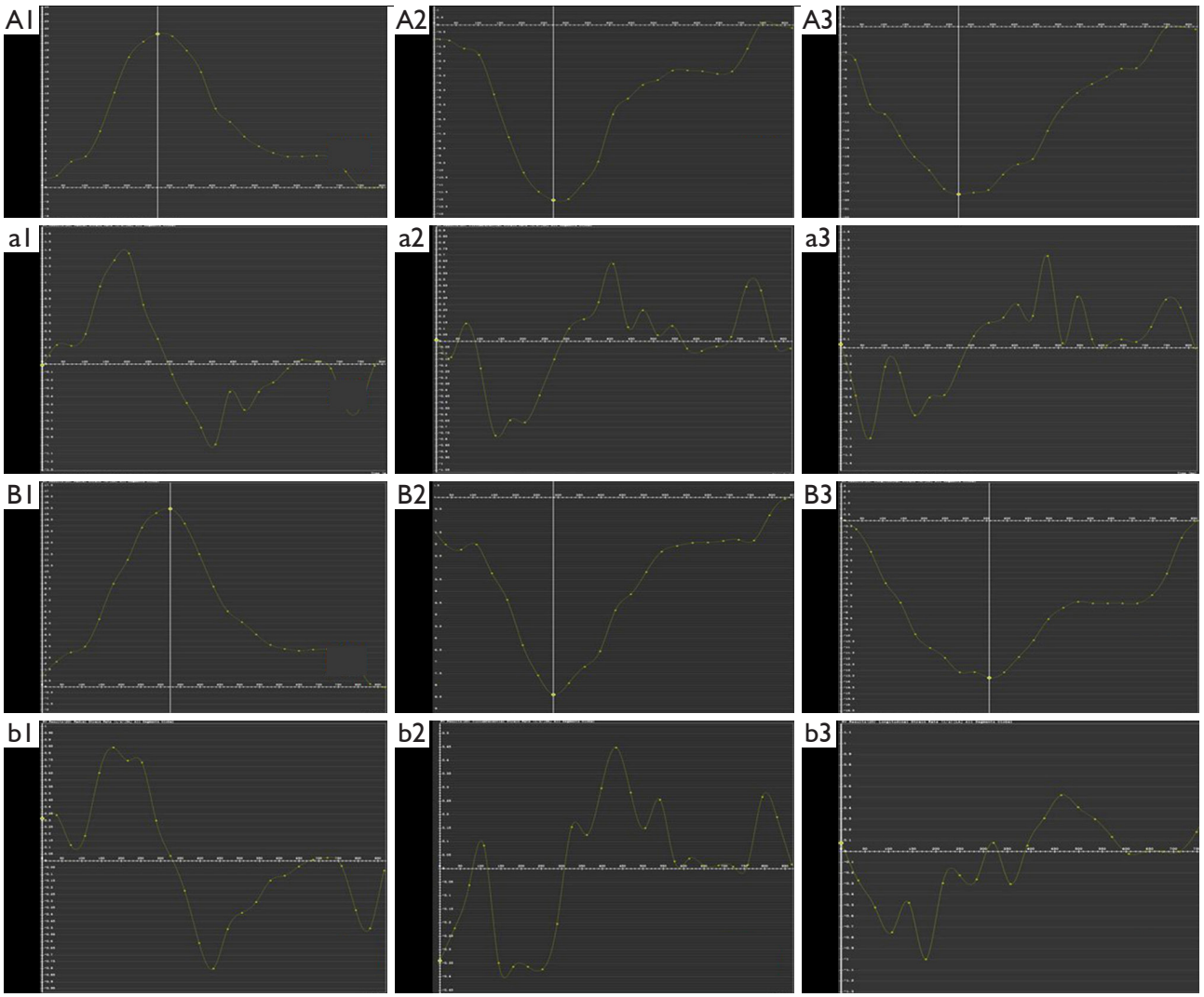

Figure 3 Measurement of RV GPS and the peak strain rate parameters in MI patients. (A1–A3) A MI (MR–) patient, (A1) GRPS =21.3%; (A2) GCPS =–12.0%; (A3) GLPS =–19.3%; (a1–a3) (a1) radial PSSR =1.4 s^{-1}, radial PDSR =–1.0 s^{-1}; (a2) circumferential PSSR =–0.8 s^{-1}, circumferential PDSR =0.6 s^{-1}; (a3) longitudinal PSSR =–1.1 s^{-1}, longitudinal PDSR =1.1 s^{-1}. (B1–B3) A MI (MR+) patient, (B1) GRPS =15.5%; (B2) GCPS =–8.4%; (B3) GLPS =–13.6%; (b1–b3) (b1) radial PSSR =0.80 s^{-1}, radial PDSR =–0.80 s^{-1}; (b2) circumferential PSSR =–0.37 s^{-1}, circumferential PDSR =0.45 s^{-1}; (b3) longitudinal PSSR =–1.00 s^{-1}, longitudinal PDSR =0.50 s^{-1}. RV, right ventricle; GPS, global peak strain; MI, myocardial infarction; MR–, without mitral regurgitation; GRPS, global radial peak strain; GCPS, global circumferential peak strain; GLPS, global longitudinal peak strain; PSSR, peak systolic strain rate; PDSR, peak diastolic strain rate.

lower than that in the control participants. On comparing the MI (MR–) group with the normal group, the GLPS and GRPS of the RV significantly decreased; however, the longitudinal peak strain rate of the RV significantly increased during the diastolic and systolic phases. Due to the RV volume and surface area considerations, a smaller inward movement of the RV was often required to achieve the same stroke volume. The decrease in the stroke volume may be attributed to the impaired radial strain of the RV. The deep muscle fibers of the RV were primarily arranged longitudinally from the base to the apex, which is potentially linked with a compensatory increase in the longitudinal strain rate during diastole and systole when the GLPS was impaired.

Table 4 Comparison of the strain parameters between RV and infarct distribution regions of LV in MI patients with different degrees of MR

Indexes	MI (MR–) (n=114)	MI (MR+, mild) (n=28)	MI (MR+, moderate) (n=37)	MI (MR+, severe) (n=20)
RV PS, %				
Radial	19.64±8.85	17.87±7.92	16.68 (10.32, 23.14)	12.36±7.71*$^{\Delta}$
Circumferential	−11.41±4.27	−10.24±4.16	−10.35±4.28	−7.73±4.31*
Longitudinal	−16.59±5.58	−16.28±5.52	−14.84±5.08	−11.65±3.50*$^{\Delta}$
RV PSSR, s^{-1}				
Radial	1.10 (0.87, 1.55)	1.05±0.39	0.94±0.42*	0.66 (0.31, 0.88)*$^{\Delta}$
Circumferential	−0.76 (−0.95, −0.62)	−0.72 (−0.88, −0.63)	−0.59±0.35*	−0.47±0.28*$^{\Delta}$
Longitudinal	−1.30 (−1.62, −0.99)	−1.04 (−1.45, −0.83)	−1.12 (−1.45, −0.84)	−0.97±0.40*
RV PDSR, s^{-1}				
Radial	−0.87 (−1.21, −0.65)	−0.82 (−0.99, −0.65)	−0.72 (−1.13, 0.44)	−0.77±0.39
Circumferential	0.59 (0.44, 0.69)	0.58 (0.45, 0.71)	0.53±0.32	0.48±0.29
Longitudinal	1.17 (0.88,1.53)	1.05 (0.74, 1.43)	0.88 (0.73, 1.48)*	0.98±0.35*
Infarct distribution regions of LV				
Anterior region	75 (65.8)	15 (53.6)	25 (67.6)	13 (65.0)
Lateral region	32 (28.1)	13 (46.4)	24 (64.9)*	12 (60.0)*
Inferior region	52 (45.6)	13 (46.4)	15 (40.5)	14 (70.0)
Infarct size, LV hyperenhancement %	24.63 (14.27, 35.04)	29.63 (21.02, 47.53)*	36.03 (24.61, 46.86)*	38.74 (23.85, 53.87)*

Data are presented as mean ± standard deviation, or the median (25th, 75th percentile), or number (percentage). *, P<0.05, MI (MR+, mild/moderate/severe) *vs.* MI (MR–) group; $^{\Delta}$, P<0.05, MI (MR+, moderate/severe) group *vs.* MI (MR+, mild) group. RV, right ventricle; LV, left ventricle; MI, myocardial infarction; MR, mitral regurgitation; MR–, without mitral regurgitation; MR+, with mitral regurgitation; PS, peak strain; PSSR, peak systolic strain rate; PDSR, peak diastolic strain rate.

Table 5 Univariate analysis of the correlation between RV peak strain and LV ejection fraction, peak strain, and MR

Indexes	RV GRPS		RV GCPS		RV GLPS	
	r	P	r	P	r	P
LVEF	0.287	0.008	0.290	0.007	0.284	0.009
LV GRPS	0.314	0.004	0.307	0.004	0.301	0.005
LV GCPS	0.367	0.001	0.347	0.001	0.338	0.002
LV GLPS	0.219	0.044	0.223	0.041	0.347	0.001
Infarct size, LV hyperenhancement %	−0.291	0.007	−0.257	0.018	−0.072	0.515
MRF, %	−0.334	0.002	−0.281	0.010	−0.283	0.009

RV, right ventricle; LV, left ventricle; MR, mitral regurgitation; GRPS, global radial peak strain; GCPS, global circumferential peak strain; GLPS, global longitudinal peak strain; LVEF, left ventricle ejection fraction; MRF, mitral regurgitation fraction.

Table 6 Multivariable analysis for the influencing factors of RV GPS and biventricular interaction in patients with MI and MR

Indexes*	RV GRPS (R^2=0.428)		RV GCPS (R^2=0.425)		RV GLPS (R^2=0.246)	
	β	P	β	P	β	P
Age	0.009	NS	0.038	NS	−0.269	0.013
Triglycerides, mmol/L	0.024	NS	−0.039	NS	−0.306	0.002
LVEF	0.033	NS	0.030	NS	−0.006	NS
MRF, %	−0.068	NS	0.011	NS	−0.073	NS
Infarct size, LV hyperenhancement %	−0.065	NS	−0.028	NS	−0.009	NS
Time from infarct to CMR	0.007	NS	0.042	NS	−0.074	NS
Inferior region	−0.024	NS	−0.004	NS	0.031	NS
Coronary artery stent	0.019	NS	−0.031	NS	0.047	NS
LV GRPS	0.095	NS	0.085	NS	0.080	NS
LV GCPS	−0.074	NS	−0.050	NS	−0.084	NS
LV GLPS	−0.027	NS	−0.032	NS	0.224	0.029
RVESV	−0.660	<0.001	−0.657	<0.001	−0.356	0.002
Smoking	−0.035	NS	−0.058	NS	0.179	NS
Hypertension	0.097	NS	0.138	NS	−0.076	NS
Diabetes mellitus	0.110	NS	0.113	NS	0.019	NS
Drinking	0.019	NS	0.028	NS	−0.103	NS

*, after adjusting for gender, BMI, SBP, and resting heart rate. RV, right ventricle; GPS, global peak strain; MI, myocardial infarction; MR, mitral regurgitation; BMI, body mass index; SBP, systolic blood pressure; GRPS, global radial peak strain; GCPS, global circumferential peak strain; GLPS, global longitudinal peak strain; β, the regression coefficient; NS, nonsignificant; LVEF, left ventricular ejection fraction; MRF, mitral regurgitation fraction; LV, left ventricle; CMR, cardiac magnetic resonance; RVESV, right ventricular end-systolic volume.

Additive damage effects of MR on RV myocardium in patients with MI

In our study, when comparing the MI (MR−) group with the MI (MR+) group, despite a larger LV MI size in the MI (MR+) group, the cardiac troponin levels were significantly lower in the MI (MR+) group (all P<0.05). This observation may be linked to variations in the timing of CMR administration in patients with MI, with levels fluctuating and returning to the baseline concentrations within a few days.

Previous research indicates that MR not only induces LV dysfunction but also contributes to RV pressure and volume overload, resulting in RV dysfunction and non-ischemic fibrosis (4). MR-associated RV dysfunction is primarily correlated with adverse LV remodeling, and ischemic MR elevates the risk of RV dysfunction (24). Changes in pulmonary circulatory resistance caused by LV MI can also impact RV function, leading to decreased RV contraction. RV myocardial dysfunction in patients with MI may be influenced by neurohormonal activation, potentially leading to ventricular remodeling (25). RV systolic function is a crucial predictor of mortality, and RV PSSR serves as a sensitive marker for detecting early RV systolic dysfunction in chronic rheumatic patients with MR (26). Lu *et al.* revealed that RV GLPS exhibited the highest association with CMR RVEF (18). In our study, the RV myocardial GPS was further impaired in the MI (MR+) group when compared to that in the MI (MR−) group. In *Table 1*, although no significant difference was noted, the time from infarct to CMR of the MI (MR+) group was relatively longer than that for the MI (MR−) group, which potentially affected the RV myocardial strain parameters. The global PSSR of the RV in the MI group with moderate-to-severe MR was further decreased when compared with that in the MI (MR−) and MI (MR+, mild) groups, leading to aggravated damage to the systolic functions of the RV.

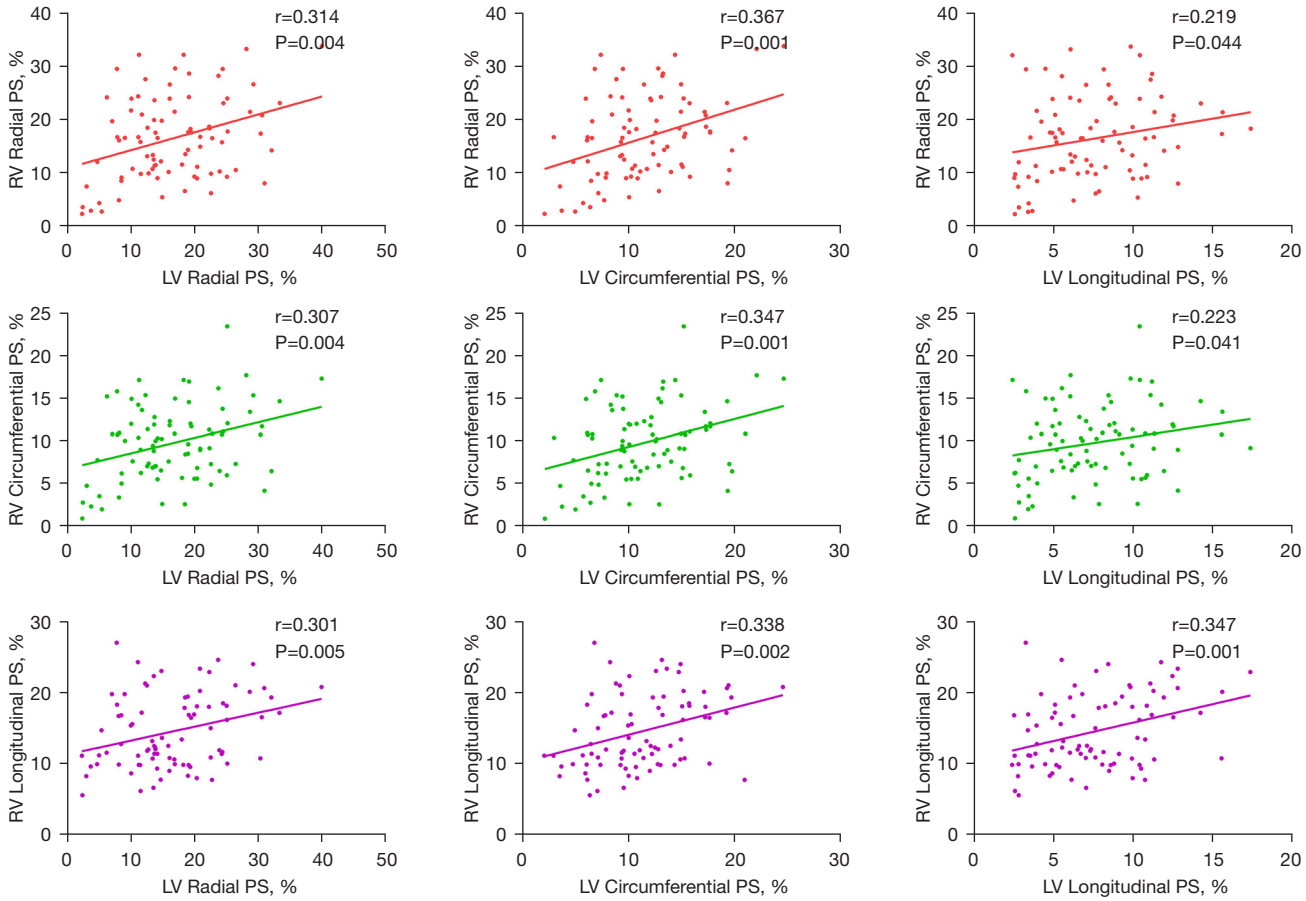

Figure 4 Correlation between RV GPS and LV GPS in patients with MI (MR+). LV, left ventricle; RV, right ventricle; PS, peak strain; GPS, global peak strain; MI, myocardial infarction; MR+, with mitral regurgitation.

Independent factors and LV and RV interaction in patients with MI and MR

Previous studies have demonstrated that age and RV global longitudinal strain are independent predictive indicators of early mortality, and RVESV has been independently associated with RV global longitudinal strain (24,27). RV GLPS serves as a robust predictive indicator for RV dysfunction (18). Anavekar *et al.* reported that decreased RV systolic function is a significant risk factor for death, stroke, and HF in patients with MI (28). Our findings thus indicate that RVESV is independently correlated with RV GPS and that age is an independent indicator of RV GLPS in patients with MI and MR. Triglycerides are associated with RV GLPS, which implies a detrimental effect of triglycerides and cholesterol remnants on the heart and longitudinal functions (29). GLPS is regarded as an early indicator of myocardial dysfunction in the majority of cardiac and pulmonary artery diseases (30).

CMR-FT can provide a quantitative assessment of the early deformation occurring in both the left and right myocardium (31,32). RV dysfunction stands as a crucial predictive indicator for adverse cardiac events and mortality (33). Subclinical systolic dysfunction in the RV has been associated with longitudinal myocardial dysfunction in the LV (34). The LV plays a pivotal role in contributing to RV ejection, with LV contraction generating 20–40% of RV stroke volume and pulmonary flow in the experimental models (35-37). The anatomic basis for LV and RV functional systolic and diastolic interdependence involves shared muscle fibers through the interventricular septum, shared epicardial circumferential myocytes, and the pericardial space (36,38). Ventricular interactions during systole and diastole are negatively influenced by RV regional inhomogeneity and the prolongation of contraction (38). Our study findings demonstrated that LV GLPS is an independent factor associated with RV GLPS.

In addition, the MR(+) group exhibited lower RVSV, indicating a biventricular interaction between the LV and RV functions.

Limitations

Although our study provided valuable insights into the associated factors of RV myocardial strain in patients with MI and MR, it has some limitations. First, being a single-center, cross-sectional, and retrospective study, inherent biases are evident that may influence the outcomes. In addition, the lack of follow-up monitoring for clinical endpoints, records of adverse cardiovascular events, and prognosis and measurement data related to the pulmonary artery are some other disadvantages. Future studies with extended follow-up and a focus on the clinical endpoints and pulmonary artery pressure measurements are necessary to further validate the conclusions of this study.

Conclusions

In conclusion, MR may compound damage to RV myocardium deformation, resulting in reduced RV strain and cardiac functions in patients with MI. LV GLPS, RVESV, triglycerides, and age emerged as independent factors that influence RV dysfunction in patients with MI and MR. The CMR-FT technology can prove valuable in monitoring the progression of RV dysfunction and myocardial peak strain damage in patients with MI and MR.

Acknowledgments

Funding: This work was financially supported by the Science and Technology Support Program of Sichuan Province of China (No. 2022NSFSC1494), and the 1·3·5 Project for Disciplines of Excellence of West China Hospital, Sichuan University (No. ZYGD18013).

Footnote

Reporting Checklist: The authors have completed the STROBE reporting checklist. Available at https://qims.amegroups.com/article/view/10.21037/qims-23-1360/rc

Conflicts of Interest: All authors have completed the ICMJE uniform disclosure form (available at https://qims.amegroups.com/article/view/10.21037/qims-23-1360/coif). The authors have no conflicts of interest to declare.

Ethical Statement: The authors are accountable for all aspects of the work in ensuring that questions related to the accuracy or integrity of any part of the work are appropriately investigated and resolved. The study was conducted in accordance with the Declaration of Helsinki (as revised in 2013). Ethical approval for this clinical study was obtained from the Biomedical Research Ethics Committee of the West China Hospital of Sichuan University (No. 2019-756). The requirement for informed consent from patients was waived due to the retrospective nature of this study.

References

1. Zhang C, Zhao L, Zhu E, Schoenhagen P, Tian J, Lai YQ, Ma X. Predictors of moderate to severe ischemic mitral regurgitation after myocardial infarction: a cardiac magnetic resonance study. Eur Radiol 2021;31:5650-8.
2. Zornoff LA, Skali H, Pfeffer MA, St John Sutton M, Rouleau JL, Lamas GA, Plappert T, Rouleau JR, Moyé LA, Lewis SJ, Braunwald E, Solomon SD; SAVE Investigators. Right ventricular dysfunction and risk of heart failure and mortality after myocardial infarction. J Am Coll Cardiol 2002;39:1450-5.
3. Ivey-Miranda JB, Almeida-Gutiérrez E, Borrayo-Sánchez G, Antezana-Castro J, Contreras-Rodríguez A, Posada-Martínez EL, González-Morales E, García-Hernández N, Romero-Zertuche D, Marquez-Gonzalez H, Saturno-Chiu G. Right ventricular longitudinal strain predicts acute kidney injury and short-term prognosis in patients with right ventricular myocardial infarction. Int J Cardiovasc Imaging 2019;35:107-16.
4. Sanders JL, Koestenberger M, Rosenkranz S, Maron BA. Right ventricular dysfunction and long-term risk of death. Cardiovasc Diagn Ther 2020;10:1646-58.
5. Tadic M, Nita N, Schneider L, Kersten J, Buckert D, Gonska B, Scharnbeck D, Reichart C, Belyavskiy E, Cuspidi C, Rottbauer W. The Predictive Value of Right Ventricular Longitudinal Strain in Pulmonary

Hypertension, Heart Failure, and Valvular Diseases. Front Cardiovasc Med 2021;8:698158.
6. Tadic M, Kersten J, Nita N, Schneider L, Buckert D, Gonska B, Scharnbeck D, Dahme T, Imhof A, Belyavskiy E, Cuspidi C, Rottbauer W. The Prognostic Importance of Right Ventricular Longitudinal Strain in Patients with Cardiomyopathies, Connective Tissue Diseases, Coronary Artery Disease, and Congenital Heart Diseases. Diagnostics (Basel) 2021.
7. Stiermaier T, Backhaus SJ, Matz J, Koschalka A, Kowallick J, de Waha-Thiele S, Desch S, Gutberlet M, Hasenfuß G, Thiele H, Eitel I, Schuster A. Frequency and prognostic impact of right ventricular involvement in acute myocardial infarction. Heart 2020. [Epub ahead of print]. doi: 10.1136/heartjnl-2020-317184.
8. Uretsky S, Gillam L, Lang R, Chaudhry FA, Argulian E, Supariwala A, Gurram S, Jain K, Subero M, Jang JJ, Cohen R, Wolff SD. Discordance between echocardiography and MRI in the assessment of mitral regurgitation severity: a prospective multicenter trial. J Am Coll Cardiol 2015;65:1078-88.
9. Thygesen K, Alpert JS, White HD; Joint ESC/ACCF/AHA/WHF Task Force for the Redefinition of Myocardial Infarction. Universal definition of myocardial infarction. J Am Coll Cardiol 2007;50:2173-95.
10. Thygesen K, Alpert JS, Jaffe AS, Simoons ML, Chaitman BR, White HD; et al. Third universal definition of myocardial infarction. J Am Coll Cardiol 2012;60:1581-98.
11. Thygesen K, Alpert JS, Jaffe AS, Chaitman BR, Bax JJ, Morrow DA, White HD; Executive Group on behalf of the Joint European Society of Cardiology (ESC)/American College of Cardiology (ACC)/American Heart Association (AHA)/World Heart Federation (WHF) Task Force for the Universal Definition of Myocardial Infarction. Fourth Universal Definition of Myocardial Infarction (2018). J Am Coll Cardiol 2018;72:2231-64.
12. Garg P, Swift AJ, Zhong L, Carlhäll CJ, Ebbers T, Westenberg J, Hope MD, Bucciarelli-Ducci C, Bax JJ, Myerson SG. Assessment of mitral valve regurgitation by cardiovascular magnetic resonance imaging. Nat Rev Cardiol 2020;17:298-312.
13. Zhang Y, Yan WF, Jiang L, Shen MT, Li Y, Huang S, Shi K, Yang ZG. Aggravation of functional mitral regurgitation on left ventricle stiffness in type 2 diabetes mellitus patients evaluated by CMR tissue tracking. Cardiovasc Diabetol 2021;20:158.
14. Krieger EV, Lee J, Branch KR, Hamilton-Craig C. Quantitation of mitral regurgitation with cardiac magnetic resonance imaging: a systematic review. Heart 2016;102:1864-70.
15. Chinitz JS, Chen D, Goyal P, Wilson S, Islam F, Nguyen T, Wang Y, Hurtado-Rua S, Simprini L, Cham M, Levine RA, Devereux RB, Weinsaft JW. Mitral apparatus assessment by delayed enhancement CMR: relative impact of infarct distribution on mitral regurgitation. JACC Cardiovasc Imaging 2013;6:220-34.
16. Bondarenko O, Beek AM, Hofman MB, Kühl HP, Twisk JW, van Dockum WG, Visser CA, van Rossum AC. Standardizing the definition of hyperenhancement in the quantitative assessment of infarct size and myocardial viability using delayed contrast-enhanced CMR. J Cardiovasc Magn Reson 2005;7:481-5.
17. Vigneault DM, te Riele AS, James CA, Zimmerman SL, Selwaness M, Murray B, Tichnell C, Tee M, Noble JA, Calkins H, Tandri H, Bluemke DA. Right ventricular strain by MR quantitatively identifies regional dysfunction in patients with arrhythmogenic right ventricular cardiomyopathy. J Magn Reson Imaging 2016;43:1132-9.
18. Lu KJ, Chen JX, Profitis K, Kearney LG, DeSilva D, Smith G, Ord M, Harberts S, Calafiore P, Jones E, Srivastava PM. Right ventricular global longitudinal strain is an independent predictor of right ventricular function: a multimodality study of cardiac magnetic resonance imaging, real time three-dimensional echocardiography and speckle tracking echocardiography. Echocardiography 2015;32:966-74.
19. Steen H, Giusca S, Montenbruck M, Patel AR, Pieske B, Florian A, Erley J, Kelle S, Korosoglou G. Left and right ventricular strain using fast strain-encoded cardiovascular magnetic resonance for the diagnostic classification of patients with chronic non-ischemic heart failure due to dilated, hypertrophic cardiomyopathy or cardiac amyloidosis. J Cardiovasc Magn Reson 2021;23:45.
20. Schmid J, Kamml C, Zweiker D, Hatz D, Schmidt A, Reiter U, Toth GG, Fuchsjäger M, Zirlik A, Binder JS, Rainer PP. Cardiac Magnetic Resonance Imaging Right Ventricular Longitudinal Strain Predicts Mortality in Patients Undergoing TAVI. Front Cardiovasc Med 2021;8:644500.
21. Abbate A, Bussani R, Sinagra G, Barresi E, Pivetta A, Perkan A, Hoke NH, Salloum FN, Kontos MC, Biondi-Zoccai GG, Vetrovec GW, Sabbadini G, Baldi F, Silvestri F, Kukreja RC, Baldi A. Right ventricular cardiomyocyte apoptosis in patients with acute myocardial infarction of the left ventricular wall. Am J Cardiol 2008;102:658-62.
22. Keskin M, Uzun AO, Hayıroğlu Mİ, Kaya A, Çınar

T, Kozan Ö. The association of right ventricular dysfunction with in-hospital and 1-year outcomes in anterior myocardial infarction. Int J Cardiovasc Imaging 2019;35:77-85.
23. Antoni ML, Scherptong RW, Atary JZ, Boersma E, Holman ER, van der Wall EE, Schalij MJ, Bax JJ. Prognostic value of right ventricular function in patients after acute myocardial infarction treated with primary percutaneous coronary intervention. Circ Cardiovasc Imaging 2010;3:264-71.
24. Kim J, Alakbarli J, Yum B, Tehrani NH, Pollie MP, Abouzeid C, Di Franco A, Ratcliffe MB, Poppas A, Levine RA, Devereux RB, Weinsaft JW. Tissue-based markers of right ventricular dysfunction in ischemic mitral regurgitation assessed via stress cardiac magnetic resonance and three-dimensional echocardiography. Int J Cardiovasc Imaging 2019;35:683-93.
25. Konishi K, Dohi K, Tanimura M, Sato Y, Watanabe K, Sugiura E, Kumagai N, Nakamori S, Nakajima H, Yamada T, Onishi K, Nakamura M, Nobori T, Ito M. Quantifying longitudinal right ventricular dysfunction in patients with old myocardial infarction by using speckle-tracking strain echocardiography. Cardiovasc Ultrasound 2013;11:23.
26. Meel R, Peters F, Libhaber E, Essop ME. Unmasking right ventricular dysfunction in chronic rheumatic mitral regurgitation. Cardiovasc J Afr 2019;30:216-21.
27. Kanar BG, Tigen MK, Sunbul M, Cincin A, Atas H, Kepez A, Ozben B. The impact of right ventricular function assessed by 2-dimensional speckle tracking echocardiography on early mortality in patients with inferior myocardial infarction. Clin Cardiol 2018;41:413-8.
28. Anavekar NS, Skali H, Bourgoun M, Ghali JK, Kober L, Maggioni AP, McMurray JJ, Velazquez E, Califf R, Pfeffer MA, Solomon SD. Usefulness of right ventricular fractional area change to predict death, heart failure, and stroke following myocardial infarction (from the VALIANT ECHO Study). Am J Cardiol 2008;101:607-12.
29. Jørgensen PG, Jensen MT, Biering-Sørensen T, Mogelvang R, Galatius S, Fritz-Hansen T, Rossing P, Vilsbøll T, Jensen JS. Cholesterol remnants and triglycerides are associated with decreased myocardial function in patients with type 2 diabetes. Cardiovasc Diabetol 2016;15:137.
30. Liu T, Wang C, Li S, Zhao Y, Li P. Age- and gender-related normal references of right ventricular strain values by tissue tracking cardiac magnetic resonance: results from a Chinese population. Quant Imaging Med Surg 2019;9:1441-50.
31. Claus P, Omar AMS, Pedrizzetti G, Sengupta PP, Nagel E. Tissue Tracking Technology for Assessing Cardiac Mechanics: Principles, Normal Values, and Clinical Applications. JACC Cardiovasc Imaging 2015;8:1444-60.
32. Huo H, Dai X, Li S, Zheng Y, Zhou J, Song Y, Liu S, Hou Y, Liu T. Diagnostic accuracy of cardiac magnetic resonance tissue tracking technology for differentiating between acute and chronic myocardial infarction. Quant Imaging Med Surg 2021;11:3070-81.
33. Roifman I, Ghugre N, Zia MI, Farkouh ME, Zavodni A, Wright GA, Connelly KA. Diabetes is an independent predictor of right ventricular dysfunction post ST-elevation myocardial infarction. Cardiovasc Diabetol 2016;15:34.
34. Todo S, Tanaka H, Yamauchi Y, Yokota S, Mochizuki Y, Shiraki H, Yamashita K, Shono A, Suzuki M, Sumimoto K, Tanaka Y, Hirota Y, Ogawa W, Hirata KI. Association of left ventricular longitudinal myocardial function with subclinical right ventricular dysfunction in type 2 diabetes mellitus. Cardiovasc Diabetol 2021;20:212.
35. Konstam MA, Kiernan MS, Bernstein D, Bozkurt B, Jacob M, Kapur NK, Kociol RD, Lewis EF, Mehra MR, Pagani FD, Raval AN, Ward C; American Heart Association Council on Clinical Cardiology; Council on Cardiovascular Disease in the Young; and Council on Cardiovascular Surgery and Anesthesia. Evaluation and Management of Right-Sided Heart Failure: A Scientific Statement From the American Heart Association. Circulation 2018;137:e578-622.
36. Sanz J, Sánchez-Quintana D, Bossone E, Bogaard HJ, Naeije R. Anatomy, Function, and Dysfunction of the Right Ventricle: JACC State-of-the-Art Review. J Am Coll Cardiol 2019;73:1463-82.
37. Lahm T, Douglas IS, Archer SL, Bogaard HJ, Chesler NC, Haddad F, et al. Assessment of Right Ventricular Function in the Research Setting: Knowledge Gaps and Pathways Forward. An Official American Thoracic Society Research Statement. Am J Respir Crit Care Med 2018;198:e15-43.
38. Naeije R, Badagliacca R. The overloaded right heart and ventricular interdependence. Cardiovasc Res 2017;113:1474-85.

Cite this article as: Wen X, Gao Y, Guo Y, Zhang Y, Zhang Y, Shi K, Li Y, Yang Z. Assessing right ventricular peak strain in myocardial infarction patients with mitral regurgitation by cardiac magnetic resonance feature tracking. Quant Imaging Med Surg 2024;14(4):3018-3032. doi: 10.21037/qims-23-1360

